

Lifeguarding Operational Camera Kiosk System (LOCKS) for Flash Rip Warning: Development and Application

Abstract

A Lifeguarding Operational Camera Kiosk System (LOCKS) is developed and implemented at the North Beach of Port Washington, WI to provide real-time flash rip warnings to beach users for the first time. LOCKS has three components. First, a real-time environmental observation system acquires timely beach view images and local environmental condition data. Second, an integrated nowcast forecast operational system, a high performance and distributed computing infrastructure, digitally detects and assesses flash rip hazards in high, moderate or low risks. Third, an automated kiosk dynamically issues real-time warnings on site by a three-color dynamic lights and a digital display monitor. Results of flash rip detection show that the combined length threshold and HSV-based segmentation method can be used in both sunny and cloudy days with an overall accuracy of 83%. Nonstationary locations and intermittent occurrences of flash rips are observed and characterized. The length of the flash rip ranges between 10 – 50 m. The duration of flash rips varies from 1 to 5 minutes with 65% of flash rips less than 2 minutes. A flash rip occurrence checklist by adding two new (storm and visual observation) factors is constructed to reliably assesses the likelihood of hazardous flash rips. Public communication through media mentions, news releases, and website usages show the strong interest and support of the LOCKS as a new approach to issue timely and dynamic flash rip warnings to beach users. LOCKS can be used to issue warnings of other types of rips like bathymetry-controlled and boundary-controlled rip currents in the future.

Keywords: flash rip, rip currents, dynamic warning, image processing, beach hazards, beach safety, meteotsunamis

1. Introduction

Flash rips, or known as transient rips, are rip currents that appear at featureless beaches (Castelle et al., 2016). Bathymetrically-controlled rip currents (Dalrymple et al., 2011), in contrast, are usually associated with morphological features including deeper channels between submerged sandbars (Reniers et al., 2006; Winter et al., 2014), offshore transverse ridges (Houser et al., 2011), sorted bedforms (Coco et al., 2007), and submarine canyon outside of surf zones (Long and Özkan-Haller, 2005). Different from stationary boundary-controlled rip currents at locations near natural headlands and anthropogenic structures (Castelle and Coco, 2013; Scott et al., 2016; Silva et al., 2010), flash rips, induced by shear instability of longshore currents (Özkan-Haller and Kirby, 1999) or migrating surfzone eddies (Feddersen, 2014), intermittently appear at nonstationary locations (Dalrymple et al., 2011). Intermittency in flash rips can be also caused by meteorologically-induced water level oscillations (MIWLO) in the Great Lakes (Linares et al., 2019; Meadows et al., 2011). Due to the nature of unpredictability, flash rips are hazardous to swimmers by unexpectedly sweeping people away from the surf zone to deeper water to cause drowning (Castelle et al., 2016; Dalrymple et al., 2011; MacMahan et al., 2006). Fatalities due to rip currents were reported globally (Gensini and Ashley, 2010). In the United States, an annual average was 58 fatalities based on incident statistics of 2008 – 2018 (National Weather Service, 2018). In the Great Lakes, a total of 185 fatalities and 591 incidents during 2002 – 2018 were recorded (Great Lake Current Incident Database, 2018). Overall, flash rips are intermittency and nonstationary at featureless beaches, imposing hidden hazards and high risks to beach users.

Warnings for rip currents to notify beach users about dangerous water conditions (Matthews et al., 2014) can influence people's decisions of entering water (White and Hyde, 2010). For example, warning signage for rip currents as part of the "Break the Grip of the Rip!" campaign

has been widely used at beaches (Brannstrom et al., 2015). Static signage for rip current warning is proven valuable for escape strategy education. Studies find that sometimes people may not be fully aware of the hazards and disasters (Houser et al., 2017). One possible reason is that the static signage is less eye-catching. Another possible cause is that users may not be able to correctly recognize the actual hazardous conditions based upon schematic illustrations on the signage (Brannstrom et al., 2015). Dynamic flags for rip current warning are thereby used by beach patrols, lifeguards, and local law enforcement officials (Brander and MacMahan, 2011; Sherker et al., 2010; White and Hyde, 2010). While the flag system has been found effective (Brannstrom et al., 2015), timely placing flags at unpatrolled beaches during rapid moving storm conditions can be challenging (Houser et al., 2017). Continuous efforts have been called for effectively issuing rip current warning, which requires reliably assessing occurrences of intermittent and nonstationary flash rips.

In the past, assessing flash rip occurrences have been conducted in several ways. First, proxies or environmental factors including wave climates, wind conditions, tidal elevations, or morphological status have been statistically correlated with or empirically related to rip current occurrences. For example, there are several rip current assessing tools like the Lushine Rip Currents scale (LURCS, Lushine, 1991), the East-Central Florida beaches scale (e.g. ECFL LURCS, Engle, 2003; Lascody, 1998; Schrader, 2004), and the Great Lakes Rip Current Checklist (GLRCC, Meadows et al., 2011). This type of assessing tools is efficient but requires site specific data and uncertainty evaluation. Second, in-situ sensors such as acoustic Doppler velocimeters or current profilers at fixed locations (Clark et al., 2010; Johnson and Pattiaratchi, 2004) can measure offshore-directed rip currents. Dense arrays of sensors at fixed locations would be required due to non-stationarity nature of flash rips (Haus, 2011). Lagrangian drifters have been employed for

tracking flash rips in the surf zone (Castelle et al., 2014; Johnson and Pattiaratchi, 2004; Scott et al., 2018). Nevertheless, use of in-situ sensors to reveal flash rips can be expensive and not practical. Third, trained lifeguards often identify presences of flash rips as sediment- or bubble-laden water jets based on visual clues of water color differences and patterns of wave breaking in surf zone (Dalrymple et al., 2011; Flo ch et al., 2018; Leatherman and Leatherman, 2017). Observations by trained lifeguards are limited to patrolled beaches, which are infeasible to achieve in all beaches. Last but not least, remote sensors like optical cameras can provide long-term observations with large field of view and required spatial-temporal resolutions (Holman et al., 2006). For example, the well-known ARGUS (Holman and Stanley, 2007), the SIRENA (Nieto et al., 2010), and COSMOS (Taborda and Silva, 2012) have been used in monitoring rip currents (Orzech et al., 2011; Radermacher et al., 2018). Studies by Murray et al. (2013) and Flo ch et al. (2018) showed that flash rips can be potentially detected based on color thresholds for rip-induced sediment plumes. To date, reliably and practically assessing the likelihood of hazardous flash rips remains a challenging research topic.

In recent years, cyberinfrastructure technology has greatly advanced to serve as an automated tool for rip current information (Alvarez-Ellacuria et al., 2009; Arun Kumar and Prasad, 2014; Voulgaris et al., 2011). For example, a Rip Risk Prediction Tool has been used to provide the hazard level of bathymetry-controlled rip currents based on forecasted flow speeds and patterns through a coupled wave and circulation model (Austin et al., 2012). Based upon the wave forecast models with the spatial resolutions >2 km on the Great Lakes (Alves et al., 2014), outlooks with three tiers of high, moderate, and low risks have been used to issue daily rip current warnings on the regional scale (<https://www.weather.gov/safety/ripcurrent-forecasts>) by the National Weather Service (NWS). Recently, a statistical model of rip current likelihood maps (Dusek and Seim,

2013), based on forecasts outputs of the higher resolution (~500 m) Nearshore Wave Prediction System (NWPS, van der Westhuysen, 2013) have been developed and validated on the U.S ocean coasts, but not yet for the Great Lakes (Churma and Churma, 2017; Moulton et al., 2017). While continuous advancements of rip current cyberinfrastructures have been made, no system with the capability of assessing the likelihood of hazardous flash rips and providing timely warnings of intermittent and nonstationary flash rips have been developed and implemented, as far as the authors are aware.

The objective of this paper is to develop and implement a Lifeguarding Operational Camera Kiosk System (LOCKS) to characterize flash rips and provide timely warnings in Lake Michigan. The LOCKS has three components. First, an integrated nowcast forecast operational system is designed and deployed to capture whole beach views and measure nearshore waves and local wind conditions. Second, an integrated nowcast forecast operational system, a high performance and distributed computing platform, is used to process acquired data and assess likelihood of flash rip occurrences. Lastly, a notifying kiosk is designed and built at the study site to deliver real-time warnings to beach users. The paper is structured as follows. The study site is described in Section 2. Section 3 details the methods including the hardware and software of the real time environmental observation system, the computing infrastructure and data processing algorithms, and the development and implementation of the kiosk and dynamic beach lights. Section 4 shows results of flash rip characteristics obtained by the LOCKS at the study site. In Section 5, possible mechanisms of flash rips, applications of the LOCKS for different types of rip currents, and public communications are discussed. Finally, summary and conclusions are given in Section 6.

2. Site Description

The study site is the North Beach at the City of Port Washington, Wisconsin, located on the western shore of Lake Michigan (see Fig. 1). The beach shoreline forms a 30-degree angle clockwise from the North. The surf zone is approximated 60 m wide away from the shoreline with a mean bottom slope of 0.04. The beach is exposed to northeast and southwest dominated winds with a mean significant wave height of 0.61 m and a mean peak wave period of 4.0 sec (WIS-USACE, 1979 – 2014). Each year the beach opens from 6 AM to 10 PM daily. Visitors and recreational water users enter the beach from two routes, as shown in the yellow dotted lines in Figure 1. One route, denoted as R1, is the lakeshore path starting from the south end of the Waste Water Treatment Plant (WWTP). The other route, denoted as R2, is the staircase path that links to the Upper Lake Park. Like many beaches in the Great Lakes, there are no lifeguards at the North Beach. Over the last several years, eight drownings and more than ten rescue incidents have been reported (GLCID, 2018; Great Lakes Surf Rescue Project, 2018). Specifically, unexpected fatalities occurred on September 2, 2012, March 16, 2016 and August 29, 2018, respectively.

3. Methods

3.1. Real Time Environmental Observation System (RTEOS)

Data acquisition including nearshore water surface images, wind conditions, and wave climates are achieved by the RTEOS with an Ethernet camera, a wind sentry, and a wave sensor, respectively. Fig. 2 shows the RTEOS components. For acquiring images, a MOBOTIX S15 Ethernet camera (see C1 in Fig. 1) is mounted on a 2-meter galvanized steel pole at a building rooftop, at approximately 30 meters above the ground and 120 meters from the North Beach entrance. A 7.9 mm focal lens with a 45° x 34° field of view with a CMOS sensor captures the

whole view of the North Beach from an oblique view. Live streaming of nearshore water is provided in continuous 1 MP videos at 2 HZ. High-resolution 6 MP images are sampled every 5 seconds. Fig. 2 shows a sample image, in which a region of interest (ROI) bounded by white solid lines. Uninterrupted power and continuous Internet are provided through a Power-Over-Ethernet (POE) switch in the WWTP building. For acquiring wind conditions, the wind sentry (see A1 in Fig. 1), a RM Young model (#03001) with a three-cup anemometer and a wind vane, is mounted on the same pole (see Fig. 2). Wind speeds and directions are sampled at 2 HZ with a 1-min average through a Campbell Scientific CR800 data logger. For acquiring wave climates, an Echologger ECT400 hydro-acoustic sounder (see W1 in Fig. 1) on an aluminum tripod frame, deployed at a water depth of approximately 3.1 meters and at 70 meters from the shore, is connected by a RS485-based protocol cable to the data logger. Wave displacements were sampled at 5 HZ and water temperatures were sampled on a 1-minute interval. The ECT400 sensor, different from the permanently installed IP camera and wind sentry, is deployed and retrieved between early June and late August for the swimming season. In addition to environmental data acquired by the RTEOS, wind data on a 10-min interval are available through a NOAA meteorological station PWA3 inside the Port Washington Harbor (see A2 in Fig. 1).

3.2. Integrated Nowcast Forecast Operational System (INFOS)

3.2.1. Computing infrastructure

General description of the INFOS is described here while the details of INFOS cyberinfrastructure can refer to Reimer and Wu (2016) and Anderson and Wu (2018). Fig. 3a shows the three components of computing infrastructure of INFOS: a locally-based High-Performance Computing (HPC) cluster, a cloud-based distributed HPC grid, and a secure web

server. The local HPC cluster, situated in the Coastal Sustainability and Environment Fluid Mechanics Lab at the University of Wisconsin – Madison, contains a master node and 128 computing nodes from eight AMD Phenom hex-core processors, a Gigabit Ethernet switch that connects to the high-speed Internet provided by the UW College of Engineering Computer-Aided Engineering (CAE) network, and an Uninterrupted Power Supply (UPS) device for power backups. The distributed HPC has a submitting server at the Center for High Throughput Computing in UW-Madison and utilizes computing nodes on the Open Science Grid (OSG). The secure web server is hosted by the CAE stack system. To schedule automated processing, MATLAB scripts are written in the master node. Recorded image snapshots and other environmental data are distributed to the local HPC computing nodes for immediate processing while the 10-min video images are submitted to the distributed HPC grids on the waiting queue to available free nodes. After computations are completed, processed data is compiled in the master node and then uploaded onto the INFOS web server. Image processing and flash rip hazard likelihood assessment are described in the following two sub-sections.

3.2.2. *Image processing*

Fig. 3b depicts the three-step image processing. In the first step, an image is segmented into regions of different morphological features - sediment plumes (SP), white-capping waves, the lake, and the land which includes trees, bluffs and other man-made structures. Note that pixels of same morphological features tend to have similar values in the Hue-Saturation-Value (*HSV*) space, which resembles closely human perceived colors. For instances, sediment plumes have hues generally less than $1/6$ and values greater than 0.5 while white-capped breaking waves have high Saturations and Values $\sqrt{S^2 + V^2} > 0.8$ (Flo ch et al., 2018). Therefore, we transform images of the Red-Green-Blue (*RGB*) color space (a Cartesian coordinate system) into those of the HSV

space (a cylindrical coordinate system), as shown in Fig. 3c. A k-means clustering method is then applied so pixels are partitioned into k segments. Afterwards, segments are identified as sediment plumes based on the HSV values of the segment centroids. At last, morphological operations by removing connected regions and small scatter pixels are performed so that flash rip features are represented.

In the second step, ortho-rectification, which transforms original oblique images into orthophotos with geo-referenced coordinates, is executed. A pin-hole camera model is assumed to describes the 2D image coordinates (x, y) in relation to 3D world coordinates (X, Y, Z) using the Direct Linear Transform (DLT) equations (Holland et al., 1997)

$$x - x_o = -f \left[\frac{m_{11}(X-X_c) + m_{12}(Y-Y_c) + m_{13}(Z-Z_c)}{m_{31}(X-X_c) + m_{32}(Y-Y_c) + m_{33}(Z-Z_c)} \right] \quad (1a)$$

$$y - y_o = -f \left[\frac{m_{21}(X-X_c) + m_{22}(Y-Y_c) + m_{23}(Z-Z_c)}{m_{31}(X-X_c) + m_{32}(Y-Y_c) + m_{33}(Z-Z_c)} \right] \quad (1b)$$

where (x_o, y_o) is the image center, (X_c, Y_c, Z_c) is the camera center, m_{ij} represents a 3 by 3 rotation matrix for the lens orientation angles, α (azimuth), τ (tilt), θ (swing), and f is the focal lens. The interior parameters (x_o, y_o) and f were calibrated using a checkerboard before the camera was installed at the study site. The exterior parameters (X_c, Y_c, Z_c) and (α, τ, θ) were calibrated (Wanek and Wu, 2006) by using 42 ground control points (GCP) surveyed with a Nikon Nivo C Series Reflector-less Total Station. Based on the DLT equations, the georeferenced (X, Y) coordinates corresponding to the image pixels (x, y) are solved by approximating a mean lake level elevation Z (Bechle et al., 2012). The orthophoto is then obtained by interpolating pixel colors for a 2D grid in world coordinates (Bechle and Wu, 2011). Fig. 3b shows that orthophotos contain geometric dimensions of segmented SPs, thus providing additional information to identify flash rips.

In the third step, detection of flash rips is achieved by meeting the two criteria: (i) a segment is identified as sediment plumes (see the pink region in Fig. 3b) and (ii) the offshore length of the sediment plume segment is greater than a threshold (see the red line in Fig. 3b). The threshold is determined by minimizing the number of discrepancies by comparing with the occurrence of flash rips perceived by human eye visualizations.

3.2.3. Flash rip hazard likelihood assessment

In this study, we assess possible occurrences of flash rips using both site-specific environmental data and image detection. Table 1 shows the Flash Rip Occurrence Checklist (FROC), adapted from the Great Lakes Rip Current Checklist (GLRCC) previously used by the NOAA NWS Great Lakes offices (Meadows et al., 2011). There are seven factors in the FROC. Four environmental factors, wind speed (U_w) in m/s, wind direction (Dir_w) in degrees (zero degree means that wind comes from the true North), nearshore significant wave height (H_s) in meter, and peak wave period (T_p) in sec, are based on local and nearshore observations, different from those based upon offshore forecasts in the GLRCC. Specific criteria of the four factors in the FROC are wind speed $U_w > 4.5$ m/s (equivalent to 10 mph), southwestern wind direction ($|Dir_w - 225| < 45^\circ$) or significant direction shift ($\Delta Dir_w > 15^\circ$ within 10 minutes), and nearshore wave condition ($H_s > 0.46$ m (equivalent to 1.5 ft) and $T_p > 3$ sec). In addition, the fifth environmental factor is the lake level change (ΔLL) referenced to the lake-wide monthly average water level of the 1985 International Great Lakes Datum (IGLD) reported in the Great Lakes Dashboard Project (Smith et al., 2016), which accounts for the effect of oscillating water levels on rip current occurrences in the closed-basin environment of the Great Lakes (Meadows et al., 2011), with the criteria $LL < -0.15$ m (equivalent to -6 in), which is modified from those used in the GLRCC. To specifically

account for the occurrence of flash rips, two new factors are added in the FROC. A storm factor considers the effects of moving storm that has crossed the Lake Michigan up to 12 hours ahead. A visual observation factor accounts for detected flash rips based on sediment plumes described in previous section. To assess the possible occurrences of hazardous flash rips, each factor is assigned with a pre-calibrated likelihood contribution in percentages, as shown in Table 1. The total likelihood (TL) of hazardous flash rips is assessed in three tiers of risk: low (L) for $TL < 40\%$, moderate (M) for $40\% \leq TL < 70\%$, and high (H) for $TL \geq 70\%$. At the L risk level, flash rips are unlikely to occur and people are safe to enter the water. At the M risk level, life-threatening flash rips are possible to occur and people are not encouraged to enter the water. At the H risk level, devastating flash rips are likely to be present and people should not enter the water.

3.3. Beach Lights and Notifying Kiosk (BLINK)

To timely issue warnings to beach users, we design and implement a Beach Lights and Notifying Kiosk (BLINK) as shown in Fig. 4. The BLINK design is highlighted in three components. First, the communication unit is an Ubiquiti's NanoBrigde RF wireless disk bridge, installed on an aluminum pole to receive wireless signals boosted from nearby buildings. Second, the control unit, connected through a POE switch to the wireless bridge, is a Raspberry Pi 3B model housed in a 50 cm by 48 cm watertight enclosure with an anti-glare screen and cooling fans. We program in Python language to recursively execute the Raspbian shell CRON task scheduler and fetch the latest flash rip information from the INFOS web server. Third, the alerting unit consists of a sun-bright 19" LCD monitor and three-color LED beacon lights. As shown in the specially designed "Rip Currents Safety Advisory" signage in Fig. 4, the LED light exhibits to the corresponding color of red, yellow or green, based on three tiers of likelihood for flash rip in high,

moderate or low occurrence, respectively. The automatic selection is achieved by a circuit that wires MOSFETs (Metal-Oxide Semiconductor Field-Effect Transistors) to the General-Purpose Input Output (GPIO) utility pins of the Raspberry Pi to control the on-and-off of each LED beacon light. Simultaneously, the monitor displays an INFOS webpage for real-time flash rip information.

Fig. 4 shows that the BLINK is constructed at the entrance to the North Beach in City of Port Washington (see K1 in Fig. 1). The BLINK are placed to the location most visible to people from the both two routes. The LED beacon lights are mounted on at a height of approximately 7.6 meter above the ground to alert visitors before entering the beach. To ensure the information displayed on the monitor readable to both adults and children users, the enclosure is installed to a height of about 1.5 m above the ground. Reliable power is provided though the nearby street light pole that connects to the City's street power system. With the established internet connectivity to the City's networks, the implementation can allow sustainable operations of the BLINK.

4. Results

4.1. Detection of Flash Rips

Detection of flash rips using different image processing methods are illustrated in three representative conditions: flash rip occurrences in a sunny day, those in a cloudy day, and no occurrence in a sunny day corresponding to the three images of 2017/07/12 16:24 PM, 2017/10/15 11:09 AM, and 2017/07/12 11:24 AM in Fig. 5 a1, a2, and a3, respectively. Results of flash rip detection by applying segmentation in the RGB color space (see Fig. 5b), segmentation in the HSV color space (see Fig. 5c), and an offshore length threshold of 15-m (represented as red solid lines) in addition to the HSV segmentation (see Fig. 5d), are compared. Note that the choice of 15-m length, determined by a dispersion relation (Sorensen, 2006) with a wave period of 4 seconds at a

water depth of 2 meters at the study site, is an approximate surf zone scale. Once wave-induced sediment plumes are beyond this threshold, flash rips are thereby detected. For flash rips in the sunny day (see the first column of Fig. 5), all three methods successfully detect flash rip-induced sediment plumes (Fig. 5b1, 5c1, and 5d1). Nevertheless, for flash rips in the cloudy day (see the second column of Fig. 5), the RGB-based segmentation fails in detecting flash rips (Fig. 5b2) since the colors of the sediment plume region appear similar to those of the lake water under low ambient lights. The HSV-based segmentation only (Fig. 5c2) and the combined length threshold and HSV segmentation (Fig. 5d2) both effectively detect flash rip-induced sediment plumes, demonstrating the advantage of using HSV colors under the low-light cloudy condition. For no flash rips in the sunny day (see the third column in Fig. 5), both the RGB-based (Fig. 5b3) and the HSV-based segmentation (Fig. 5c3) detect wave breaking-induced sediments which have similar color characteristics as those of flash-rip induced sediment plumes. The combined length threshold and HSV-based segmentation (Fig. 5c3) can check if the sediment plumes have an elongated shape caused by flash rips, yielding no false detection. In short, the RGB-based segmentation is capable of detecting flash rip in sunny days. The HSV-based segmentation can be used to detect flash rips in both sunny and cloudy days with low ambient lighting. By adding the length threshold, the false alarms of flash rips in sunny days can be avoided.

Statistics of flash rip detection using the three image processing methods are calculated and compared here. Table 2 shows the percentages of three outcomes: correct detection, false alarm, and miss. Correct detection is counted when the flash rip detection is in consistent with that viewed by human visual observation. False alarm is counted when flash rip is falsely identified in the image but not perceived by human eyes (e.g. Fig. 5b3 or 5c3). Miss is counted when flash rip is not detected in the image but are perceived by human eyes (e.g. Fig. 5b2). In the column of the

correct detection, the RGB segmentation has a 55% accuracy compared to the greatly improved 75 % accuracy of the HSV segmentation. Adding the length threshold further improves the accuracy to 83%. In the column of false alarm, errors of the three methods show a similar trend. Particularly, adding the length threshold effectively reduces false alarm with the lowest percentage of 8%. In the column of miss, percentage errors for the three methods indicate the advantage of the HSV-based segmentation and the combined method to reliably detect flash rip under sunny and cloudy conditions. Overall, the statistics for flash rip detection using the RGB-based and the HSV-based segmentation methods in this study supports the previous results that flash rips can be detected based on color thresholds for rip-induced sediment plumes (Murray et al., 2013, Flo ch et al., 2018). The combined length threshold and HSV segmentation method further improves flash rip detection, consistent to human eye observations. To apply the image-based method to other beaches, the length threshold can be determined by local nearshore conditions including wave climates, beach slope, and surf zone depth. Furthermore, the threshold can be adjusted by examining captured images for complexity of color features, average color tones of sediment plumes in water, and potential view obstructions from land or human structures.

4.2. Location of Flash Rips

Spatial occurrences of flash rips are nonstationary, as shown on the orthophotos in Fig. 6. Flash rip-induced sediment plumes occurred at various locations in the Region Of Interest (ROI) that spans 500 m in the longshore x direction and 50 m in the cross-shore y direction y (see Fig. 2). For instances, two flash rips (red arrows in Fig. 6a) occurred at $x = 150$ m and $x = 200$ m at 14:34 PM on July 12, 2017; three (see Fig. 6b) occurred at $x = 125$ m, $x = 190$ m and $x = 250$ m at 16:24 PM on the same day; and eight (see Fig 6c) occurred at multiple locations from $x = 25$ m

to $x = 400$ m at 11:49 AM on August 3, 2017, indicating that the occurrence of flash rips were not fixed. For a total of 152 images with flash rip detected, the calculated occurrence frequency of flash rips with 5m x 5m spatial grid resolution over the ROI is shown in Fig. 6 (d). The frequency of occurrences in all cells within $y < 25$ m are larger than zero, indicating that flash rips occurred everywhere. Overall, several notes are drawn here. First, images recorded from the Ethernet camera can be effectively rectified through the INFOS image processing to reveal the locations of flash rip-induced sediment plumes. Second, occurrences of flash rips are ubiquitous but hotspots of flash rips at the study site have been identified, at locations $x = 120$ m to $x = 150$ m and $y = 20$ m based on the highest probability of 48%. Third, the spacing between flash rips can range from 20 m to 60 m. Last but not least, flash rip-induced sediment plumes identified within the ROI can range from 10 m beyond the surf zone to a distance greater than 50m (equivalent to a length of a standard long course swimming pool) in Lake Michigan, comparable to 50 ~ 100 m reported in oceanic coastal areas (Flo ch et al., 2018).

4.3. Duration of Flash Rips

Intermittency of occurred flash rips are examined here. We calculate the durations (T) from the images acquired by the RTEOS. For example, flash rip-induced sediment plumes occurred at 14:17:04 PM on July 12, 2017 (Fig. 7a1) and were gone at 14:18:14 PM for a duration of 70-sec (Fig. 7a2). Another example shows that flash rips started at 16:44:04 PM (Fig. 7b1) and were no longer visible at 16:49:09 PM (see Fig. 7b2), yielding a duration of $T = 305$ seconds. Statistics of flash rip durations in Fig. 7c. Overall, several findings are noticed. First, the image acquisition protocol of the Ethernet camera shows the capability to capture the intermittent occurrences of flash rips. The durations of each flash rip can thereby be reliably obtained. Second, 65% of flash

rips had the duration less than 2 minutes, comparable to the 60% oceanic flash rips reported by Floch et al. (2018). Third, approximately 5 % of flash rips had the duration longer than 5 minutes. Fourth, the maximum, average, and minimum durations are found to be 345 seconds, 115 seconds, and 30 seconds, respectively, indicating that flash rips have a short-lifespan and decay after a few minutes. The statistics are consistent to those by Slattery (2010) and Murray et al. (2013). Last but not least, flash rips tend to occur on and off many times throughout the same day, suggesting that water users in Lake Michigan should be cautious about not only intermittency but also recurrence of flash rips.

4.4. Likelihood of Flash Rip Hazards

The likelihood of flash rip hazards is assessed based upon the FROC. For example, the time series of the total likelihood (TL) and the seven factors in the assessment matrix for July 12, 2017 event are plotted in Fig. 8. At 14:17 PM, a H risk tier of flash rip is assessed at 95 % total likelihood (TL) with 30 % contributed from the visual observation factor of flash rips identified in the image (Fig. 8b), 15 % from the storm factor (Fig. 8c), and 50 % from the four local environmental factors - wind speed $U_w = 5.2$ m/s (Fig. 8d) and direction from SW of $Dir_w = 221^\circ$ (Fig. 8c), significant wave height $H_s = 0.61$ m (Fig. 8e), wave period $T_p = 5.0$ sec (Fig. 8g), but no contribution from lake level change of < 0.15 m (Fig. 8h). At 16:44 PM, a M risk tier is assessed at 65 % TL with 30 % from the visual observation factor, 15 % from the storm factor, and 20 % from the wave factor ($H_s = 0.64$ m and $T_p = 5.1$ sec). Shortly after, at 16:49 PM, an L risk tier is assessed at 35% with 15 % from the storm factor and the 20 % from the wave factors ($H_s = 0.55$ m and $T_p = 4.7$ sec). The results of likelihood flash rip hazards (Fig. 8) assessed by the FROC are consistent to the human-eye observed occurrence from the events on July 12, 2017 (Fig. 7a1 and 7b1) and other days (not shown here for brevity) including at 11:09 AM on Oct 15, 2017 (Fig 5a2)

and at 11:40 AM on Aug 3, 2017 (Fig. 6c). Note that for our study site sediment plumes are used as visual observation for flash rip identification. For beaches where sediment plumes may not be available, we suggest using other indicative visual signatures such as water foams and bubbles (Leatherman and Leatherman, 2017). Overall, the Flash Rip Occurrence Checklist provides a tool for reliably and practically assessing the likelihood of hazardous flash rips in Lake Michigan for the first time, as far as the authors are aware.

4.5. Real-time Warning of Flash Rips

In this study, timely warnings of intermittent and nonstationary flash rips have been developed and implemented as the Beach Lights and Notifying Kiosk (BLINK). Specifically, at the entrance to the North Beach in City of Port Washington, the BLINK provides the real-time flash rip warning on the webpage (<http://infosportwashington.cee.wisc.edu/Northbeachwatch1.html>). Fig. 9 shows an example of flash rips at 14:29 PM on July 12, 2017. At the top of the page, the assessed flash rip risk is “HIGH” in bolded texts with the text color in red. If assessed risk is moderate or low level, bolded texts would accordingly be changed to yellow or green, respectively. Underneath, a table with detailed explanations about three tiers of risk of flash rips is provided. Wordings in the table are adapted from those used in rip current forecasts by the NOAA National Weather Service (<https://www.weather.gov/safety/ripcurrent-forecasts>). On the left is the real-time view of the North Beach from the RTEOS camera. A message that alerts users of watching out for sediment plumes is overlaid at the bottom of on the image. The text background and the image border are shown in red, yellow or green accordingly. At the page bottom left, a table summarizes the latest environmental conditions including wave height, period, wind speed and direction, and air temperature. At the bottom right, safety recommendations and the “flip, float and follow”

escape strategy (Great Lakes Surf Rescue Project, 2018) in graphics are displayed. Overall, the BLINK provides a real-time flash rip warning with color that is consistent to that used in the dynamic flag system. In addition, text explanation, visual and environmental conditions, and safety recommendation allow beach users to learn about flash rip hazards and escape strategy. The real-time BLINK, based on outcomes of the reliable assessments of flash rip likelihood, provides a new approach for the first time to issue flash rip warnings to beach users effectively.

5. Discussion

5.1. Mechanisms for Flash Rips

Two mechanisms for generating flash rips have been reported in literature. First, shear instabilities of longshore currents (Castelle et al., 2016; Özkan-Haller and Kirby, 1999) under obliquely incident waves can generate unsteady vortices, resulting in locally strong and narrow offshore-directed out-bursting flows as transient and nonstationary rips (Castelle et al., 2014; Feddersen, 2014). Flash rips observed on Aug 3, 2017 (Fig. 10a) could possibly be caused by this mechanism as observed waves approached to shore at wave height of 0.67 m, wave period of 6.3 sec, and wave angle at approximately 20° (Fig. 10b). Second, alongshore variation of vorticity caused by the passage of breaking and nonbreaking regions of short-crest waves under normal incident angle (Clark et al., 2012; Peregrine, 1998) can cascade into large-scale surf zone eddies (Feddersen, 2014; Spydell et al., 2009), leading to episodic and unpredictable bursts of water jetting offshore (Castelle et al., 2016; Johnson and Pattiaratchi, 2006). Flash rips observed on March 30, 2017 (Fig. 10c) could likely be related to this mechanism as the detected sediment plume (red arrow in Fig. 10d) is located right in the gap between of two wave crests, with a near-normal incidence and approximated wave height of 1.8 m and wave period of 7.1 sec.

A new mechanism to generate flash rips associated with meteorological-induced water level oscillations (MIWLO) in the Lake Michigan has been recently reported by Linares et al. (2019). Specifically, meteotsunamis, one type of MIWLO with periods ranging from a few minutes to 2 hours, are propagating waves generated by fast moving atmospheric disturbances in barometric pressure or wind (Bechle et al., 2016; Monserrat et al., 2006). Bechle and Wu (2014) investigated the large MIWLO of 1954 meteotsunami event that caused seven people drownings. Anderson et al. (2015) reported that the large nearshore currents of meteotsunamis generated by two convective storms swept three swimmers about 0.5 miles offshore in Lake Erie. Linares et al. (2019) revealed that unexpected rip currents can be caused by rapidly receding water levels and generated vorticities in strong longshore currents. In this study, we summarize flash rip currents dates and images, wave characteristics (H_s and T_p), wind speed (U_w) and direction (Dir_w), and radar reflectivity images obtained from NOAA National Climatic Data Center in Table 3. It is of interest that eight out of the nine flash rip days are associated with moving atmospheric storm disturbances. For example, Fig. 10e shows an image of flash rip-induced sediment plumes on July 21, 2017. The maximum height of water level oscillations was 0.57 m around 10:20 AM, as shown in Fig. 10f. Using the wavelet power spectrums (Linares et al., 2016), the period of the water level oscillation at the time was 15 minutes, as shown in Fig. 10 (g). Based upon storm type classification described in (Bechle et al., 2015), a bow type storm had crossed the Lake Michigan and reached Port Washington around the same time. All these characteristics meet the criteria (Bechle et al., 2015; Linares et al., 2016) to be a meteotsunami-induced water level fluctuation event. The co-occurrence of the meteotsunami events and flash rips suggest that the mechanism described by Linares et al. (2019) could possibly be the cause for observed flash rips. Future study should investigate the roles of MIWLO and associated processes in generating flash rips.

5.2. Other Types of Rip Currents

Two other types of rip currents at the study site are observed. First, potential locations of bathymetry-controlled rips are obtained by processing recorded RTEOS images. Specifically, we employ the time-averaged (or timex) imaging technique (Holman et al., 2006; Holman and Stanley, 2007) to identify rip channels as the darker region located in between brighter regions that represent sandbars due to depth-limited wave breaking. Fig. 11a shows a daily timex orthophoto on Aug 11, 2016. Two oblique rip channels (at $x \approx 145$ m and at $x \approx 185$ m) in the gaps between three curved sandbars at 10-20 m offshore are clearly observed. The daily timex orthophoto on Sep 14, 2016 (Fig. 11b) shows that the rip channels had entirely disappeared and were replaced by a long and straight bar at about 20 m offshore. At later time, the daily timex orthophoto on Oct 11, 2016 (Fig. 11c) shows that a new rip channel formed (at $x \approx 170$ m) in the gap of a single bar and doubled bars. The dynamic evolution of sandbars suggests the possible occurrence of bathymetry-controlled rip currents at the study site. Second, boundary-controlled rip currents are observed using another camera with field of view towards the breakwater of the Port Washington Harbor on Jun 5, 2017, as shown in Fig. 11d. Rip-induced sediment plumes were along the coastal breakwater (red solid arrow) and near the shore towards the breakwater (red dashed arrow). The incident waves were propagating in a highly oblique angle, as shown in black arrow in Fig. 11e. The observed rips were likely caused by wave-generated longshore currents (Longuet-Higgins, 1970) being deflected when encountering the rigid breakwater structure, resulting in the offshore-directed currents (Dalrymple et al., 2011; Wind and Vreugdenhil, 1986). Overall, observations using the camera in the RTEOS reveal several types of rip current occurrences, which may explain eight drownings and more than ten rescue incidents at Port Washington, WI during the last several years.

5.3. Public Communications

Media mentions and news releases on local (City of Port Washington, Ozaukee Press, Milwaukee Journal Sentinel) and regional (UW Sea Grant, Phy.org) channels have greatly promoted the usages of LOCKS by residents and visitors. Outcomes of public communications are summarized here based upon usage statistics in three perspectives. First, page views of the INFOS website (<http://infosportwashington.cee.wisc.edu/>), tracked by Google Analytics, show a monthly average of 9,650 page views since the website was online in September 2015. A maximum 34,200 page views was reached in August 2016 shortly after several media mentions and news releases. In 2017 and 2018, monthly page views in beach season months maintained at 16,500 and at 19,000 respectively, indicating continuous public uses and interests in rip current safety information. Second, user behaviors are inferred based upon usage logs on when and how the INFOS webpages were accessed. In terms of time, heavy loads of views were usually in early mornings starting at 6 AM on Fridays, Saturdays and Sundays. It is conjectured that people likely checked the water information before they made the decision to go to the beach. In terms of devices, 61 % views were made from desktops and tablets versus 39% from mobile devices, supporting the previous conjecture that people were likely at home when they accessed the information. As we see that large amounts of INFOS usages were made beforehand, which could be up to hours ahead of when people were actually at the beach, BLINK as the in-situ device can be of great help to provide the most updated information about the dangerous rip current conditions. Last but not least, BLINK usages, tracked by a nearby security camera, show that the daily maximum of 55 visits and the average of 20 visits were achieved in May, 2019. In each visit, the number of people ranged from 1 person to up to 5 people. Approximately 30% of total tracked visits were families with young children. 75% of people passing by had stopped to check the monitor, showing that BLINK can

attract people to notice any potential dangerous rip current and water conditions. With these user statistics, the LOCKS has not only shown the continuous public interests and needs for timely water condition, but also demonstrated that BLINK can be an effective approach to issue rip current warnings.

6. Summary and Conclusion

The Lifeguarding Operational Camera Kiosk System (LOCKS) is developed and implemented at the North Beach on Lake Michigan in City of Port Washington, WI. The three components of the LOCKS are the real time environmental observation system for data acquisition, the Integrated Nowcast Forecast Operational System (INFOS) for image and data processing, and the Beach Lights and Notifying Kiosk for timely and dynamic warnings of flash rips. Results of flash rip detection show that the combined length threshold and HSV-based segmentation method can be used in both sunny and cloudy days with an overall accuracy of 83%, better than the RGB-based or HSV-based segmentation methods. Nonstationary locations and intermittent occurrences of flash rips in Lake Michigan are observed and characterized for the first time. Flash rip-induced sediment plumes can range from 10 m beyond the surf zone to a distance greater than 50 m. The spacing between flash rips can range from 20 m to 60 m. Flash rips tend to occur on and off many times throughout the same day. The duration of flash rips varies from 1 to 5 minutes with 65% of flash rips less than 2 minutes, indicating that flash rips have a short-lifespan and decay after a few minutes. Consistent to human-eye observed occurrences, the Flash Rip Occurrence Checklist including both environmental factors and two new (storm and visual observation) factors reliably assesses the likelihood of hazardous flash rips. The methodology presented in this paper can be employed to other beaches by adjusting thresholds based upon local nearshore wave conditions

and the visual observation factor like bubbles. The design of the Beach Lights and Notifying Kiosk system employs automated three-color LED beacon lights that mimics the dynamic flag system used by beach patrols. The dynamic lights and kiosk, implemented at the entrance to the North Beach most visible to beach users, can provide real-time water conditions and issue warnings of potential dangerous flash rips. Public communication through media mentions, news releases, and website usages show the strong interest and support of the LOCKS as a new approach to effectively issue flash rip warnings to beach users for the first time. The LOCKS can be further used to issue warnings of other types of dangerous currents including bathymetry-controlled and boundary-controlled rips, which were also observed in this study. Future study is suggested to reveal the co-occurrence of meteotsunamis and flash rips and investigate the roles of meteorologically induced water level oscillations and associated processes in generating flash rips.

Acknowledgement

This study and the LOCKS were supported by the National Oceanic and Atmospheric Administration (NOAA) Coastal Storms Program, Wisconsin Coastal Management Program (WCMP), University of Wisconsin Sea Grant Institute (UW-Sea Grant), and gift funds from WE Energies and local friends of Port Washington group. The authors specially thank Mr. Tom Malda, former Mayor of City of Port Washington, for his vision to develop the cyberinfrastructure to ensure rip current warning for beach safety. We would like to thank Mr. Todd Breiby, Mr. Michael Friis, and Ms. Angel Kathleen from WCMP for funding the beach lights and kiosk system and their support in coordination, education, and outreach for rip current safety. We also thank Mr. Gene Clark, a coastal specialist from UW Sea Grant, for providing valuable knowledge related to nearshore processes near coastal structures. In addition, Ms. Moira Harrington and Ms. Marie

Zhuikov at UW-Sea Grant for their dedication to communicating rip current hazards to the Great Lakes community are acknowledged. Outreach activities related to the NOAA rip current rip current outlook by Mr. Marc Kavinsky, Lead Forecaster of Marine Program Leader at NOAA-National Weather Service – Milwaukee/Sullivan, are noted and acknowledged. Last but not least, the authors acknowledge Mr. Marty Becker, Ms. Kiley Schulte, Mr. Dennis Cherny, Mr. Dan Buehler, Mr. Charlie Imig, Ms. Lisa Rathke, Mr. Randy Tetzlaff, and many staff at the City of Port Washington, WI for the assistances in deployment and operation of the LOCKS.

References

- Alvarez-Ellacuria, A., Orfila, A., Olabarrieta, M., Gómez-pujol, L., Medina, R., Tintoré, J., 2009. An Alert System for Beach Hazard Management in the Balearic Islands. *Coast. Manag.* 37, 569–584. <https://doi.org/10.1080/08920750903150662>
- Alves, J.-H.G.M., Chawla, A., Tolman, H.L., Schwab, D., Lang, G., Mann, G., Alves, J.-H.G.M., Chawla, A., Tolman, H.L., Schwab, D., Lang, G., Mann, G., 2014. The Operational Implementation of a Great Lakes Wave Forecasting System at NOAA/NCEP*. *Weather Forecast.* 29, 1473–1497. <https://doi.org/10.1175/WAF-D-12-00049.1>
- Anderson, E.J., Bechle, A.J., Wu, C.H., Schwab, D.J., Mann, G.E., Lombardy, K.A., 2015. Reconstruction of a meteotsunami in Lake Erie on 27 May 2012: Roles of atmospheric conditions on hydrodynamic response in enclosed basins. *J. Geophys. Res. Ocean.* 120, 8020–8038. <https://doi.org/10.1002/2015JC010883>
- Anderson, J.D., Wu, C.H., 2018. Development and application of a real-time water environment cyberinfrastructure for kayaker safety in the Apostle Islands, Lake Superior. *J. Great Lakes Res.* 44, 990–1001. <https://doi.org/10.1016/J.JGLR.2018.07.006>
- Arun Kumar, S.V. V., Prasad, K.V.S.R., 2014. Rip current-related fatalities in India: a new predictive risk scale for forecasting rip currents. *Nat. Hazards* 70, 313–335. <https://doi.org/10.1007/s11069-013-0812-x>
- Austin, M.J., Scott, T.M., Russell, P.E., Masselink, G., 2012. Rip Current Prediction: Development, Validation, and Evaluation of an Operational Tool. *J. Coast. Res.* 29, 283. <https://doi.org/10.2112/JCOASTRES-D-12-00093.1>
- Bechle, A.J., Wu, C.H., 2014. The Lake Michigan meteotsunamis of 1954 revisited. *Natural Hazards.* 74(1), 155–177. <https://doi.org/10.1007/s11069-014-1193-5>
- Bechle, A.J., Kristovich, D.A.R., Wu, C.H., 2015. Meteotsunami occurrences and causes in Lake Michigan. *J. Geophys. Res. Ocean.* 120, 8422–8438. <https://doi.org/10.1002/2015JC011317>
- Bechle, A.J., Wu, C.H., 2011. Virtual wave gauges based upon stereo imaging for measuring surface wave characteristics. *Coast. Eng.* 58, 305–316. <https://doi.org/10.1016/J.COASTALENG.2010.11.003>
- Bechle, A.J., Wu, C.H., Kristovich, D.A.R., Anderson, E.J., Schwab, D.J., Rabinovich, A.B., 2016. Meteotsunamis in the Laurentian Great Lakes. *Sci. Rep.* 6, 37832. <https://doi.org/10.1038/srep37832>
- Bechle, A.J., Wu, C.H., Liu, W.-C., Kimura, N., 2012. Development and Application of an Automated River-Estuary Discharge Imaging System. *J. Hydraul. Eng.* 138, 327–339. [https://doi.org/10.1061/\(ASCE\)HY.1943-7900.0000521](https://doi.org/10.1061/(ASCE)HY.1943-7900.0000521)
- Brander, R.W., MacMahan, J.H., 2011. Future Challenges for Rip Current Research and Outreach, in: Leatherman, S., Fletemeyer, J. (Eds.), *Rip Currents: Beach Safety, Physical Oceanography, and Wave Modeling*. CRC Press, pp. 1–29.
- Brannstrom, C., Lee Brown, H., Houser, C., Trimble, S., Santos, A., 2015. “You can’t see them from sitting here”: Evaluating beach user understanding of a rip current warning sign. *Appl. Geogr.* 56, 61–70. <https://doi.org/10.1016/J.APGEOG.2014.10.011>
- Castelle, B., Almar, R., Dorel, M., Lefebvre, J.-P., Senechal, N., Anthony, E.J., Laibi, R., Chuchla, R., Penhoat, Y. du, 2014. Rip currents and circulation on a high-energy low-tide-terraced beach (Grand Popo, Benin, West Africa). *J. Coast. Res.* 70, 633–638. <https://doi.org/10.2112/SI70-107.1>

- Castelle, B., Coco, G., 2013. Surf zone flushing on embayed beaches. *Geophys. Res. Lett.* 40, 2206–2210. <https://doi.org/10.1002/grl.50485>
- Castelle, B., Scott, T., Brander, R.W., McCarroll, R.J., 2016. Rip current types, circulation and hazard. *Earth-Science Rev.* 163, 1–21. <https://doi.org/10.1016/J.EARSCIREV.2016.09.008>
- Churma, M.E., Churma, M.E., 2017. Observation Methodologies for NOAA Operational Rip Current Forecast Models.
- Clark, D.B., Elgar, S., Raubenheimer, B., 2012. Vorticity generation by short-crested wave breaking. *Geophys. Res. Lett.* 39, 2012GL054034. <https://doi.org/10.1029/2012GL054034>
- Clark, D.B., Feddersen, F., Guza, R.T., 2010. Cross-shore surfzone tracer dispersion in an alongshore current. *J. Geophys. Res.* 115, C10035. <https://doi.org/10.1029/2009JC005683>
- Coco, G., Murray, A.B., Green, M.O., Thieler, E.R., Hume, T.M., 2007. Sorted bed forms as self-organized patterns: 2. Complex forcing scenarios. *J. Geophys. Res.* 112, F03016. <https://doi.org/10.1029/2006JF000666>
- Dalrymple, R.A., MacMahan, J.H., Reniers, A.J.H.M., Nelko, V., 2011. Rip Currents. *Annu. Rev. Fluid Mech.* 43, 551–581. <https://doi.org/10.1146/annurev-fluid-122109-160733>
- Dusek, G., Seim, H., 2013. A Probabilistic Rip Current Forecast Model. *J. Coast. Res.* 289, 909–925. <https://doi.org/10.2112/JCOASTRES-D-12-00118.1>
- Engle, J., 2003. Formulation of a rip current forecasting technique through statistical analysis of rip current-related rescues. Univ. Florida.
- Feddersen, F., 2014. The Generation of Surfzone Eddies in a Strong Alongshore Current. *J. Phys. Oceanogr.* 44, 600–617. <https://doi.org/10.1175/JPO-D-13-051.1>
- Flo ch, F., Mabilia, G.R., Almar, R., Castelle, B., Hall, N., Du Penhoat, Y., Scott, T., Delacourt, C., 2018. Flash Rip Statistics from Video Images. *J. Coast. Res.* 81, 100–106. <https://doi.org/10.2112/SI81-013.1>
- Gensini, V.A., Ashley, W.S., 2010. An examination of rip current fatalities in the United States. *Nat. Hazards* 54, 159–175. <https://doi.org/10.1007/s11069-009-9458-0>
- Great Lake Current Incident Database, 2018 Swim Season: Rip Current and Channel Current Incident Summary. <http://www.crh.noaa.gov/mqt/?n=glcidyearlystats,2018> (accessed 27 May 2019).
- Great Lakes Surf Rescue Project, Great Lakes Drownings. <http://www.glsrp.org/statistics/>, 2018 (accessed 27 May 2019).
- Haus, B.K., 2011. Remote sensing applied to rip current forecasts and identification, in: Leatherman, S., Fletemeyer, J. (Eds.), *Rip Currents: Beach Safety, Physical Oceanography, and Wave Modeling*. CRC Press, pp. 133–146.
- Holland, K.T., Holman, R.A., Lippmann, T.C., Stanley, J., Plant, N., 1997. Practical use of video imagery in nearshore oceanographic field studies. *IEEE J. Ocean. Eng.* 22, 81–92. <https://doi.org/10.1109/48.557542>
- Holman, R.A., Stanley, J., 2007. The history and technical capabilities of Argus. *Coast. Eng.* 54, 477–491. <https://doi.org/10.1016/J.COASTALENG.2007.01.003>
- Holman, R.A., Symonds, G., Thornton, E.B., Ranasinghe, R., 2006. Rip spacing and persistence on an embayed beach. *J. Geophys. Res.* 111, C01006. <https://doi.org/10.1029/2005JC002965>
- Houser, C., Barrett, G., Labude, D., 2011. Alongshore variation in the rip current hazard at Pensacola Beach, Florida. *Nat. Hazards* 57, 501–523. <https://doi.org/10.1007/s11069-010-9636-0>

- Houser, C., Trimble, S., Brander, R., Brewster, B.C., Dusek, G., Jones, D., Kuhn, J., 2017. Public perceptions of a rip current hazard education program: “Break the Grip of the Rip!” *Nat. Hazards Earth Syst. Sci.* 17, 1003–1024. <https://doi.org/10.5194/nhess-17-1003-2017>
- Johnson, D., Pattiaratchi, C., 2006. Boussinesq modelling of transient rip currents. *Coast. Eng.* 53, 419–439. <https://doi.org/10.1016/J.COASTALENG.2005.11.005>
- Johnson, D., Pattiaratchi, C., 2004. Transient rip currents and nearshore circulation on a swell-dominated beach. *J. Geophys. Res.* 109, C02026. <https://doi.org/10.1029/2003JC001798>
- Lascody, R.L., 1998. EAST CENTRAL FLORIDA RIP CURRENT PROGRAM, National Weather Digest.
- Leatherman, S.P., Leatherman, S.B., 2017. Techniques for Detecting and Measuring Rip Currents. *Int. J. Earth Sci. Geophys. Cit. Leatherman SB 2017*, 14.
- Linares, Á., Bechle, A.J., Wu, C.H., 2016. Characterization and assessment of the meteotsunami hazard in northern Lake Michigan. *J. Geophys. Res. Ocean.* 121, 7141–7158. <https://doi.org/10.1002/2016JC011979>
- Linares, Á., Wu, C.H., Bechle, A.J., Anderson, E.J., Kristovich, D.A.R., 2019. Unexpected rip currents induced by a meteotsunami. *Sci. Rep.* 9, 2105. <https://doi.org/10.1038/s41598-019-38716-2>
- Long, J.W., Özkan-Haller, H.T., 2005. Offshore controls on nearshore rip currents. *J. Geophys. Res.* 110, C12007. <https://doi.org/10.1029/2005JC003018>
- Longuet-Higgins, M.S., 1970. Longshore currents generated by obliquely incident sea waves: 1. *J. Geophys. Res.* 75, 6778–6789. <https://doi.org/10.1029/JC075i033p06778>
- Lushine, J.B., 1991. A Study of Rip Current Drownings and Related Weather Factors. NATL. WEA. DIG 13--19.
- MacMahan, J.H., Thornton, E.B., Reniers, A.J.H.M., 2006. Rip current review. *Coast. Eng.* 53, 191–208. <https://doi.org/10.1016/J.COASTALENG.2005.10.009>
- Matthews, B., Andronaco, R., Adams, A., 2014. Warning signs at beaches: Do they work? *Saf. Sci.* 62, 312–318. <https://doi.org/10.1016/J.SSCI.2013.09.003>
- Meadows, G., Purcell, H., Guenther, D., Meadows, L., Kinnunen, R.E., Clark, G., 2011. Rip Currents in the Great Lakes: An Unfortunate Truth, in: Leatherman, S., Fletemeyer, J. (Eds.), *Rip Currents: Beach Safety, Physical Oceanography, and Wave Modeling*. CRC Press, pp. 199–214.
- Monserrat, S., Vilibić, I., Rabinovich, A.B., 2006. Meteotsunamis: atmospherically induced destructive ocean waves in the tsunami frequency band. *Nat. Hazards Earth Syst. Sci.* 6, 1035–1051. <https://doi.org/10.5194/nhess-6-1035-2006>
- Moulton, M., Dusek, G., Elgar, S., Raubenheimer, B., Moulton, M., Dusek, G., Elgar, S., Raubenheimer, B., 2017. Comparison of Rip Current Hazard Likelihood Forecasts with Observed Rip Current Speeds. *Weather Forecast.* 32, 1659–1666. <https://doi.org/10.1175/WAF-D-17-0076.1>
- Murray, T., Cartwright, N., Tomlinson, R., 2013. Video-imaging of transient rip currents on the Gold Coast open beaches. *J. Coast. Res.* 165, 1809–1814. <https://doi.org/10.2112/SI65-306.1>
- National Weather Service. Natural Hazard Statistics – Weather Fatalities 2018. <https://www.nws.noaa.gov/om/hazstats.shtml>, 2018 (accessed 27 May 2019).
- Nieto, M.A., Garau, B., Balle, S., Simarro, G., Zarruk, G.A., Ortiz, A., Tintoré, J., Álvarez-Ellacuría, A., Gómez-Pujol, L., Orfila, A., 2010. An open source, low cost video-based coastal monitoring system. *Earth Surf. Process. Landforms* 35, 1712–1719.

- <https://doi.org/10.1002/esp.2025>
- Orzech, M.D., Reniers, A.J.H.M., Thornton, E.B., MacMahan, J.H., 2011. Megacusps on rip channel bathymetry: Observations and modeling. *Coast. Eng.* 58, 890–907. <https://doi.org/10.1016/J.COASTALENG.2011.05.001>
- Özkan-Haller, H.T., Kirby, J.T., 1999. Nonlinear evolution of shear instabilities of the longshore current: A comparison of observations and computations. *J. Geophys. Res. Ocean.* 104, 25953–25984. <https://doi.org/10.1029/1999JC900104>
- Peregrine, D.H., 1998. Surf Zone Currents. *Theor. Comput. Fluid Dyn.* 10, 295–309. <https://doi.org/10.1007/s001620050065>
- Radermacher, M., de Schipper, M.A., Reniers, A.J.H.M., 2018. Sensitivity of rip current forecasts to errors in remotely-sensed bathymetry. *Coast. Eng.* 135, 66–76. <https://doi.org/10.1016/J.COASTALENG.2018.01.007>
- Reimer, J.R., Wu, C.H., 2016. Development and Application of a Nowcast and Forecast System Tool for Planning and Managing a River Chain of Lakes. *Water Resour. Manag.* 30, 1375–1393. <https://doi.org/10.1007/s11269-016-1228-7>
- Reniers, A.J.H.M., MacMahan, J.H., Thornton, E.B., Stanton, T.P., 2006. Modelling infragravity motions on a rip-channel beach. *Coast. Eng.* 53, 209–222. <https://doi.org/10.1016/J.COASTALENG.2005.10.010>
- Schrader, M., 2004. EVALUATION OF THE MODIFIED ECFL LURCS RIP CURRENT FORECASTING SCALE AND CONDITIONS OF SELECTED RIP CURRENT EVENTS IN FLORIDA.
- Scott, T., Austin, M., Masselink, G., Russell, P., 2016. Dynamics of rip currents associated with groynes — field measurements, modelling and implications for beach safety. *Coast. Eng.* 107, 53–69. <https://doi.org/10.1016/J.COASTALENG.2015.09.013>
- Scott, T., Castelle, B., Almar, R., Senechal, N., Floch, F., Detandt, G., 2018. Controls on Flash Rip Current Hazard on Low-Tide Terraced Tropical Beaches in West Africa. *J. Coast. Res.* 81, 92. <https://doi.org/10.2112/SI81-012.1>
- Sherker, S., Williamson, A., Hatfield, J., Brander, R., Hayen, A., 2010. Beachgoers' beliefs and behaviours in relation to beach flags and rip currents. *Accid. Anal. Prev.* 42, 1785–1804. <https://doi.org/10.1016/J.AAP.2010.04.020>
- Silva, R., Baquerizo, A., Losada, M.Á., Mendoza, E., 2010. Hydrodynamics of a headland-bay beach—Nearshore current circulation. *Coast. Eng.* 57, 160–175. <https://doi.org/10.1016/J.COASTALENG.2009.10.003>
- Slattery, M.P., 2010. Assessing the nature of rip currents along the south shore of Long Island, NY: Dominant rip type and insights into possible forcing mechanisms. The Graduate School, Stony Brook University: Stony Brook, NY.
- Smith, J.P., Hunter, T.S., Clites, A.H., Stow, C.A., Slawewski, T., Muhr, G.C., Gronewold, A.D., 2016. An expandable web-based platform for visually analyzing basin-scale hydro-climate time series data. *Environ. Model. Softw.* 78, 97–105. <https://doi.org/10.1016/J.ENVSOF.2015.12.005>
- Sorensen, R.M., 2006. *Basic Coastal Engineering (Third Edition)*, Springer, New York. 324pp
- Spydell, M.S., Feddersen, F., Guza, R.T., 2009. Observations of drifter dispersion in the surfzone: The effect of sheared alongshore currents. *J. Geophys. Res.* 114, C07028. <https://doi.org/10.1029/2009JC005328>
- Taborda, R., Silva, A., 2012. COSMOS: A lightweight coastal video monitoring system. *Comput. Geosci.* 49, 248–255. <https://doi.org/10.1016/J.CAGEO.2012.07.013>

- van der Westhuysen, A.J., 2013. Development and validation of the Nearshore Wave Prediction System.
- Voulgaris, G., Kumar, N., Warner, J.C., 2011. Methodology for prediction of rip currents using a three-dimensional numerical, coupled, wave current model, in: Leatherman, S., Fletemeyer, J. (Eds.), *Rip Currents: Beach Safety, Physical Oceanography, and Wave Modeling*. CRC Press, pp. 107–124.
- Wave Information Studies – United States Army Corps of Engineers. Lake Michigan (1979-2014). <http://wis.usace.army.mil/hindcasts.html> (accessed 27 May 2019)
- Wanek, J.M., Wu, C.H., 2006. Automated trinocular stereo imaging system for three-dimensional surface wave measurements. *Ocean Eng.* 33, 723–747. <https://doi.org/10.1016/J.OCEANENG.2005.05.006>
- White, K.M., Hyde, M.K., 2010. Swimming between the flags: A preliminary exploration of the influences on Australians' intentions to swim between the flags at patrolled beaches. *Accid. Anal. Prev.* 42, 1831–1838. <https://doi.org/10.1016/J.AAP.2010.05.004>
- Wind, H.G., Vreugdenhil, C.B., 1986. Rip-current generation near structures. *J. Fluid Mech.* 171, 459. <https://doi.org/10.1017/S0022112086001520>
- Winter, G., van Dongeren, A.R., de Schipper, M.A., van Thiel de Vries, J.S.M., 2014. Rip currents under obliquely incident wind waves and tidal longshore currents. *Coast. Eng.* 89, 106–119. <https://doi.org/10.1016/J.COASTALENG.2014.04.001>

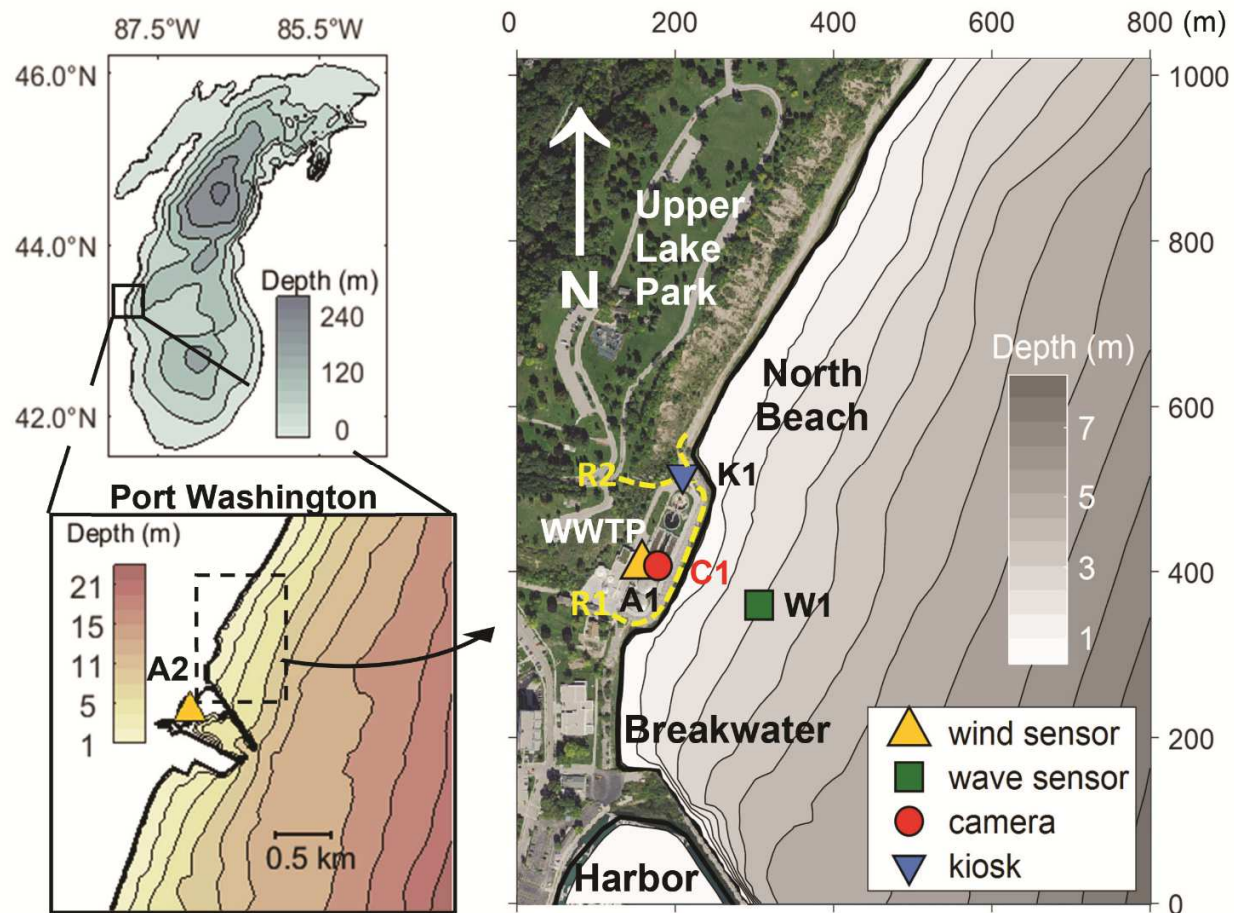


Fig. 1. The North Beach in Lake Michigan at Port Washington, WI. The two zoom-in map view show locations of two wind sensors A1 and A2 (orange triangle), a wave sensor W1 (green square), an Ethernet camera C1 (red dot), and a kiosk K1 (blue flipped triangle). Two routes to access the North Beach are shown in yellow dotted lines. Bathymetry are represented by the depth contours and color bars.

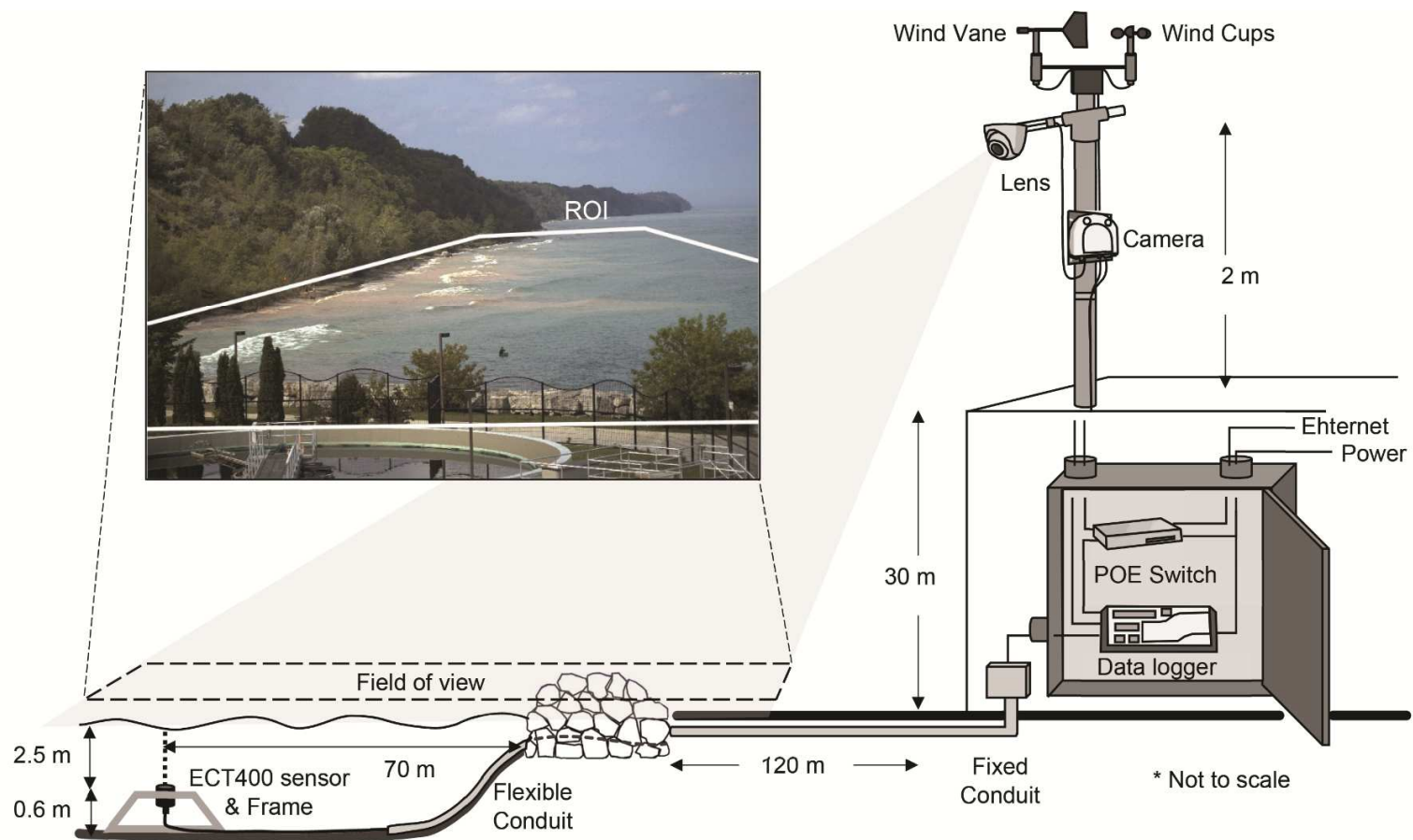


Fig. 2. The Real Time Environmental Observation System (RTEOS) consists of an Ethernet camera, a wind sentry on the rooftop, and an ECT 400 wave sensor deployed underwater connected to a data logger and a PoE switch for power and data transfer. The embedded image, a snapshot acquired at 2017/07/12 16:24 PM, shows flash rip-induced sediment plumes within a region of interest (ROI) defined by white solid lines.

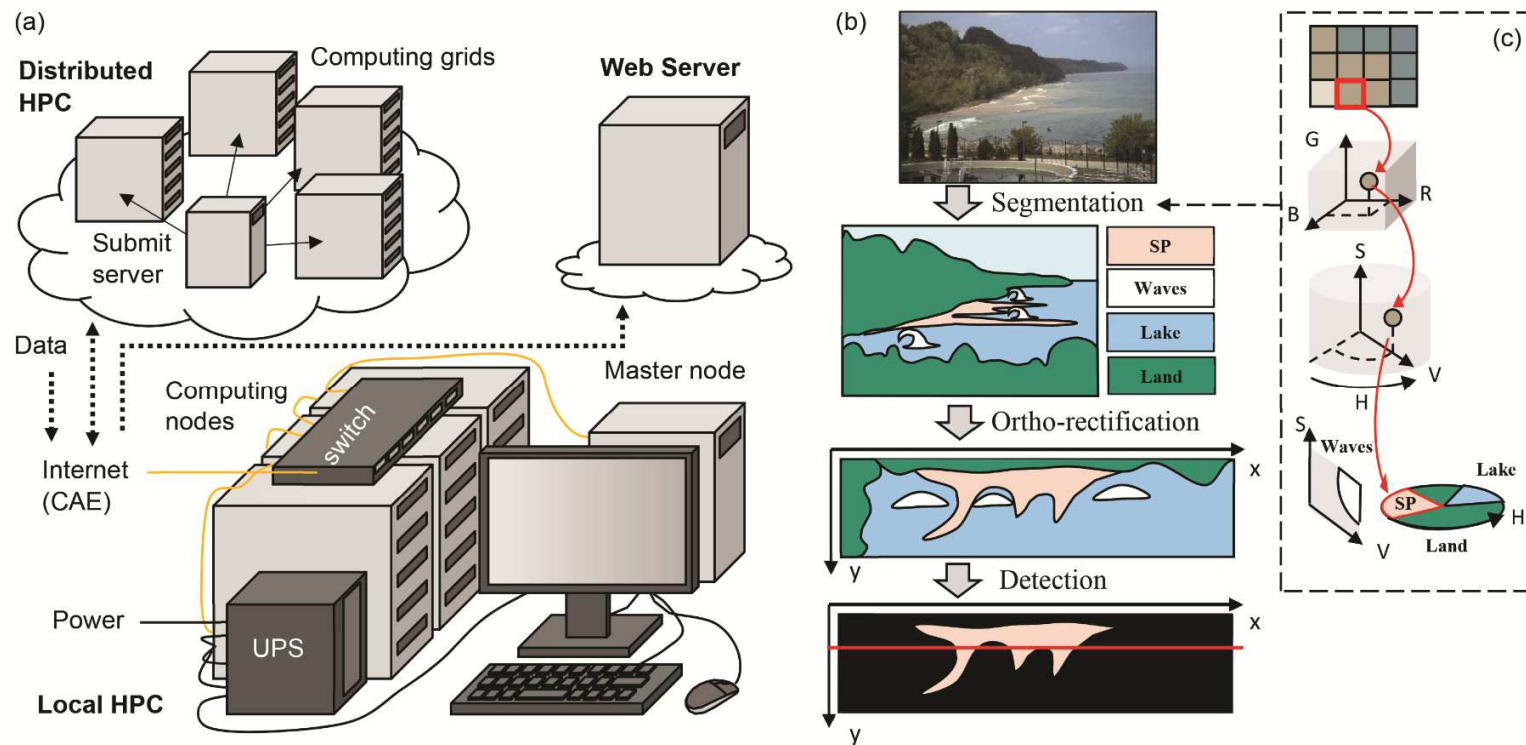


Fig. 3. (a) Computing infrastructure of the Integrated Nowcast Forecast Operation System (INFOS) consists of a local HPC, a distributed HPC, and a web server. (b) Three-step image processing of INFOS are segmentation, ortho-rectification, and flash rip detection. (c) In segmentation step, each pixel is transformed from RGB values to HSV values.

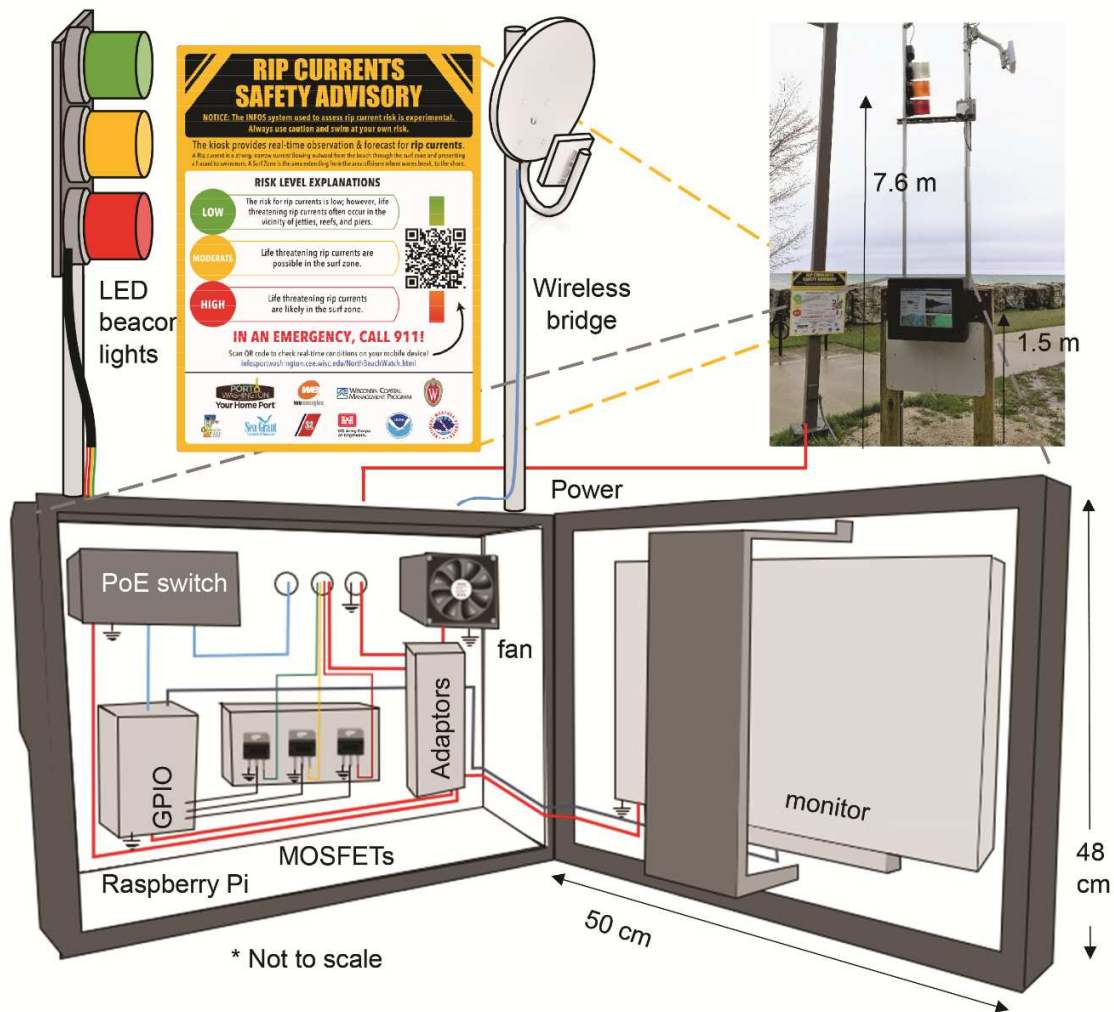


Fig. 4. Beach lights and Notifying Kiosk (BLINK) with three components: a communication unit consists of a wireless bridge; a control unit consists of a Raspberry Pi connected through a PoE to the wireless bridge, housed in the enclosure; and an alerting unit consists of a digital LCD monitor in the enclosure and a three-color LED beacon lights. A “Rip Current Safety Advisory” signage is attached to a light pole by the BLINK.

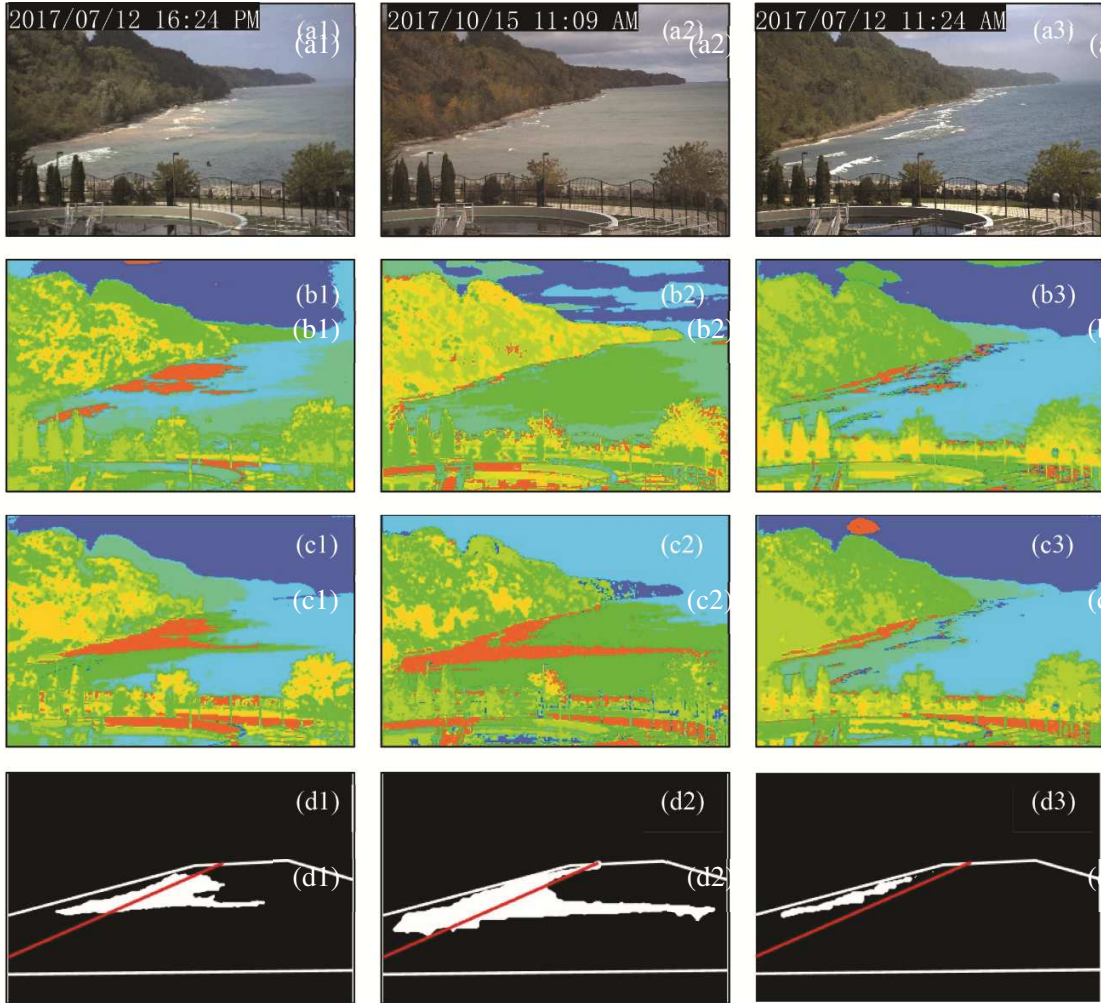


Fig. 5. Detection of flash rips under three representative conditions: (a1) flash rips in a sunny day at 16:24 PM, 2017/07/12; (a2) flash rips in a cloudy day at 11:09 AM, 2017/10/15; (a3) no flash rip in a sunny day at 11:24 AM, 2017/07/12 by using (b) RGB color space segmentation, (c) HSV color space segmentation, and (d) HSV color space segmentation and the length threshold (red solid lines) in ROI (white solid lines).

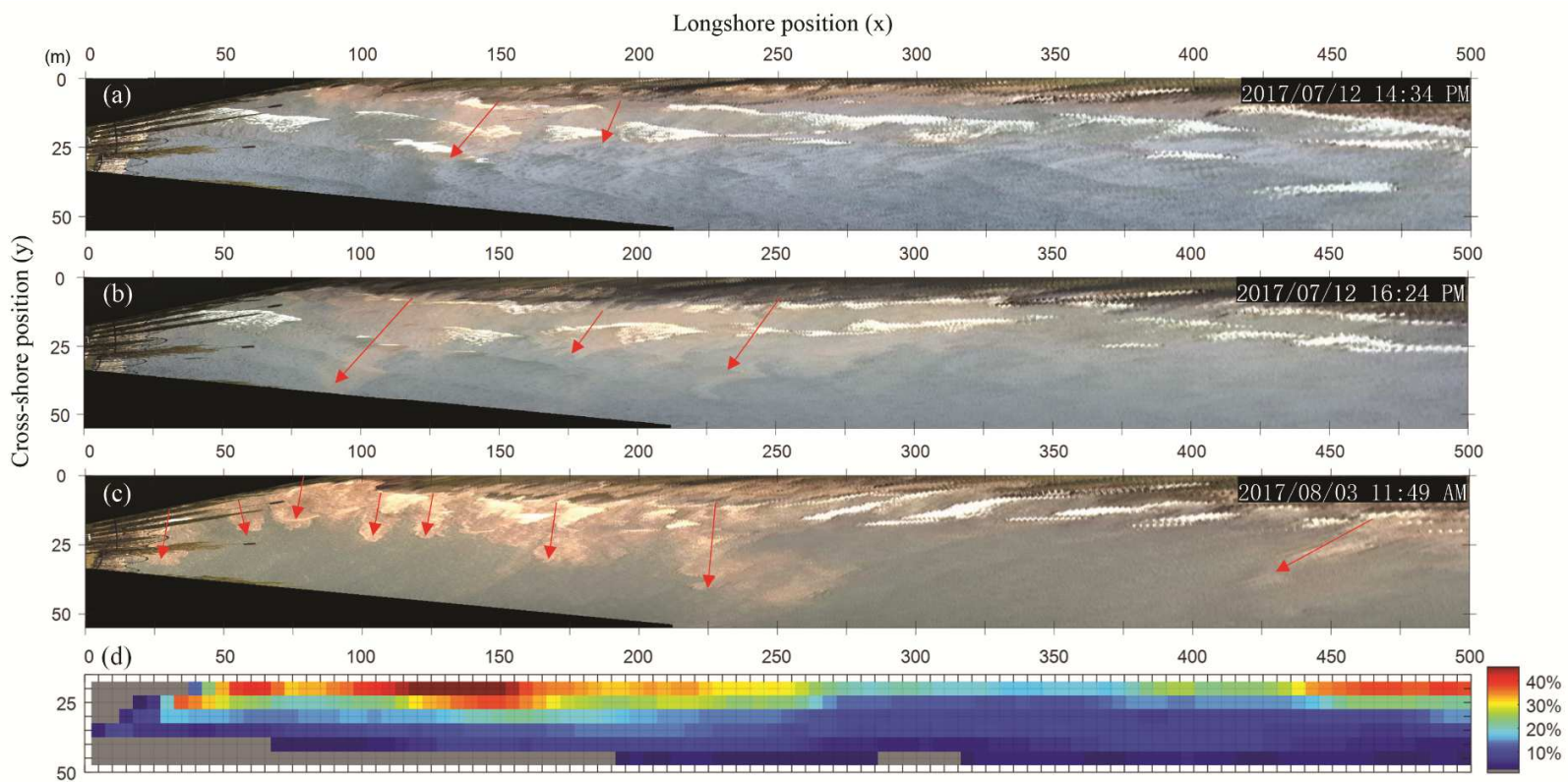


Fig. 6. Orthophotos for the ROI of images at (a) 14:34 PM on July 12, 2017, (b) 16:24 PM on July 12, 2017, and (c) 11:49 AM on August 3, 2017 with red arrows representing locations of flash rip-induced sediment plumes. (d) Frequency occurrence of flash rips at 5m by 5m spatial grid resolution spanning over the ROI.

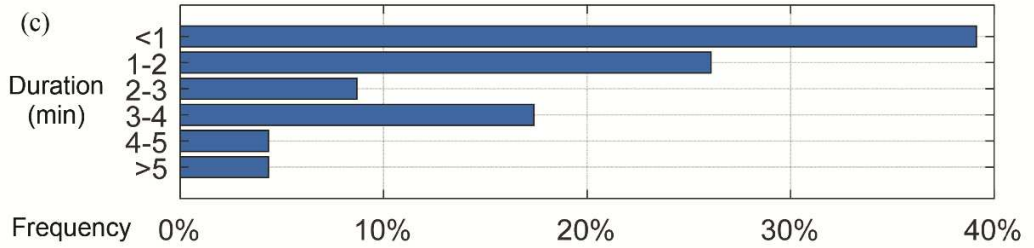


Fig. 7. Two examples of flash rips with (a) a short duration of $T = 70$ sec and (b) a long duration of $T = 305$ sec. (c) the frequency histogram of flash rip durations at a 1-minute bin interval.



Fig. 8. Likelihood of flash rip hazards on July 12, 2017: (a) total likelihood (TL) ranging from 0 to 100%, and the three tiers of risk in high (red), moderate (yellow), and low (green); (b) image observation factor, with 1 (red) for flash rips detected in the image and 0 (blue) otherwise; (c) storm factor, with 1 (red) for storm occurred in the past 12 hours and 0 (blue) otherwise; (d-h) five environmental factors: wind speed U_w , wind direction Dir_w , wave height H_s , wave period T_p , and lake level change ΔLL . Red shading represents criteria met and the red dots in (e) represent shifting wind criterion met. Percentage contributions of each factor are labeled on right side of axis.

Flash Rip Risk is now **HIGH**

Webcam



Watch out for sediment plumes, they indicate dangerous flash rips!

Explanation

LOW	Flash rips are not expected. Always use caution and never swim alone.
MODERATE	Flash rips are expected. Always have a flotation device with you in the water.
HIGH	Life-threatening flash rips are expected. Wind and/or wave conditions support flash rips to form.

Conditions

Update at: **2017/07/12 14:29 PM**

Wave Height	2.1 ft	Wave Period	5.1 sec
Water Temp (surf)	55.2 °F	Water Temp. (bot)	50.1 °F
Wind Speed	13.2 mph	Wind Direction	SSW
Air Temp	83.2 °F	Air Pressure	29.9 in Hg

Safety

Never Swim Alone

Watch Children Closely

When in Doubt, Don't Go Out!

DROWNING? THEN FLIP, FLOAT, AND FOLLOW!

Flip over onto your back and float.

Float face:

- Keep head above water.
- Take your feet down from bar and panic, don't panic.
- Conserve your energy.

Follow the safest course to safety:

- Turned right the current.
- Follow the current to allow itself into the rip.
- Flowing, swim perpendicular to the flow.
- Use head to sides, continue floating and try to signal for help.

SAND BAR

GLYPHONG

Fig. 9. Real-time display of the BLINK shows a high risk of flash rips at 14:29 PM on July 12, 2017. The display consists of a webcam view, a table for risk level explanation, a table for real-time environmental conditions, and safety advisory.

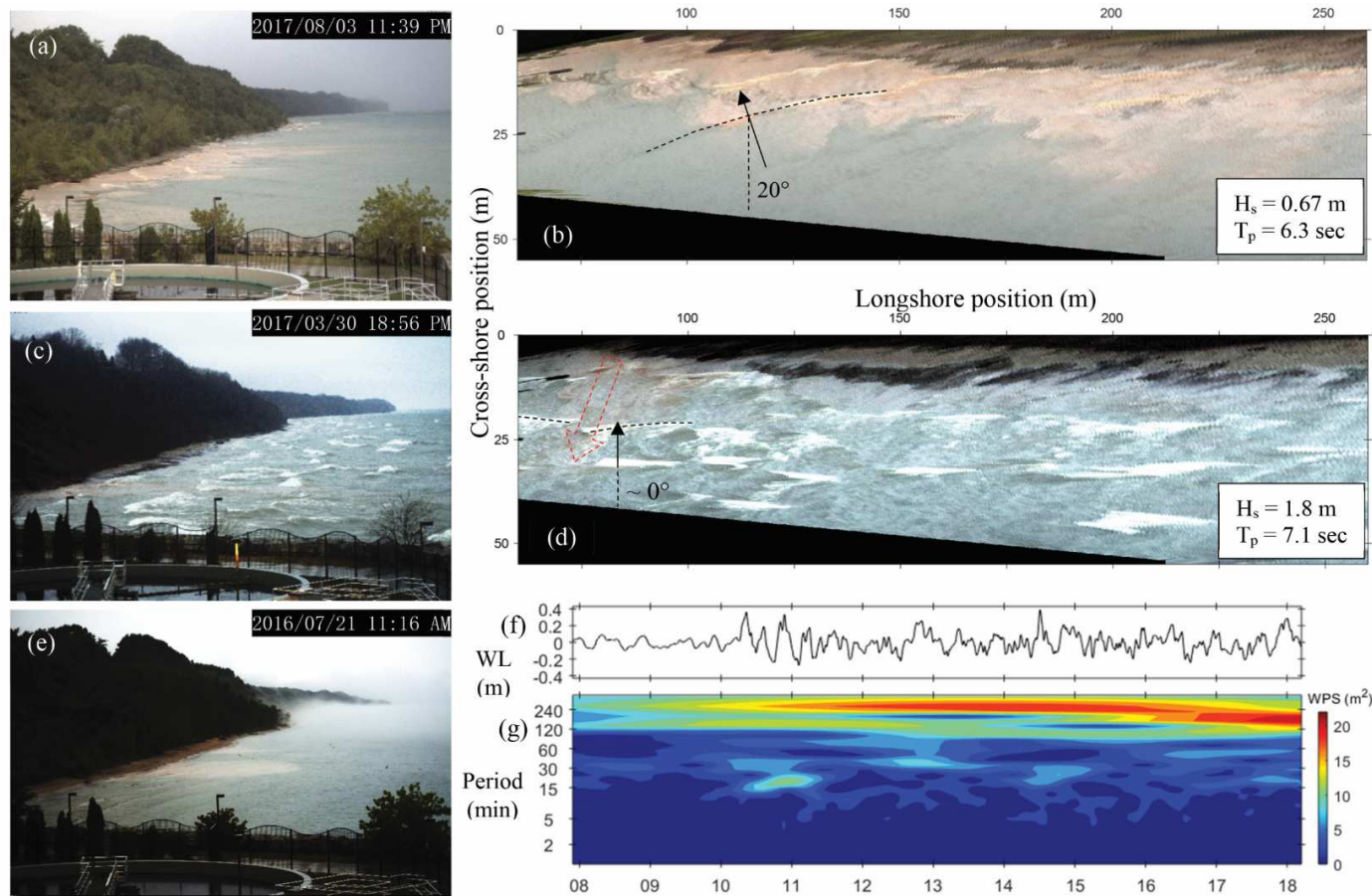


Fig. 10. (a) An oblique image shows shear instability induced flash rips at 11:39 PM on Aug 3, 2017 and (b) the corresponding orthophoto shows the incident wave angle of 20° . (c) An oblique image shows vorticity of breaking short-crest waves induced flash rips at 18:56 PM on Mar 3, 2017 and (d) the corresponding orthophoto shows sediment plumes between crests of shore-normal incidence waves. (e) An oblique image shows MIWLO-induced flash rips at 11:16 AM on Jul 21, 2017. (f) The time series of water level displacements on Jul 21, 2017 and (g) the corresponding wavelet power spectrum shows a meteotsunami event at 10:30 AM with maximum height of 0.57 m and periods of 15 min.

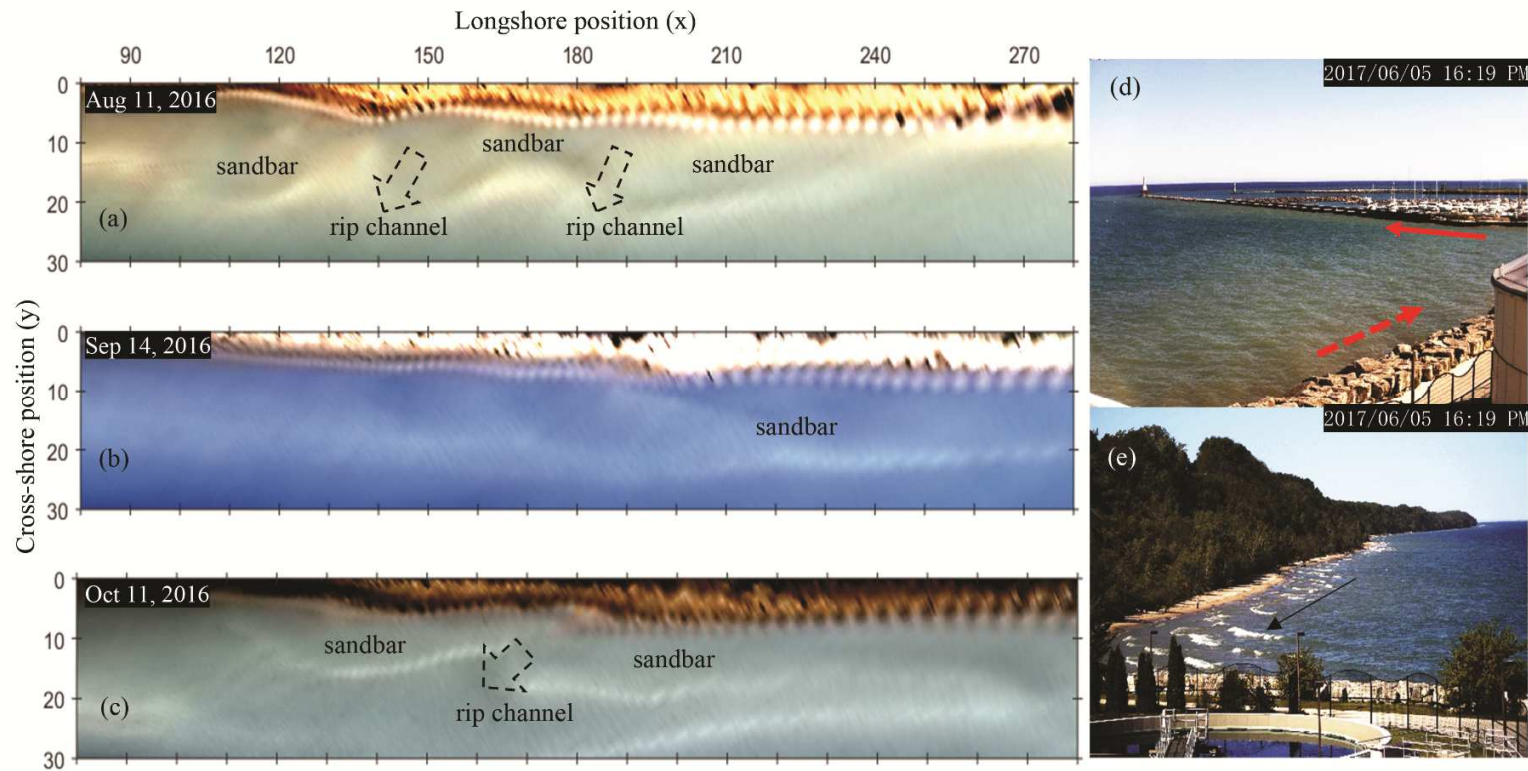


Fig. 11. Daily timex orthorectified images show three time stamps: (a) two rip channels (black dotted arrows) on Aug 11, 2016 as potential locations for bathymetry-controlled rip currents, (b) the channels disappeared on Sep 14, and (c) a new formed rip channel on Oct 11, 2016. (d) An oblique image acquired by the RTEOS camera with a field of view towards the Breakwater shows sediment plumes induced by boundary-controlled rip currents (red solid arrow) on Jun 5, 2017, likely due to deflection of longshore currents (red dashed arrow) at the breakwater. (e) An oblique image of the North Beach shows wave propagating in highly oblique incidence (black arrow).

Table 1. Flash Rip Occurrence Checklist (FROC)








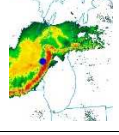

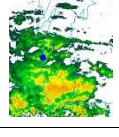

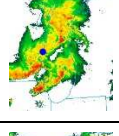



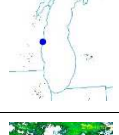

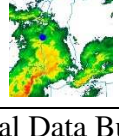
Factors	Criteria	Likelihood
U_w	$U_w > 4.5 \text{ m/s (10 mph)}$	15 %
Dir_w	$ \text{Dir}_w - 225 < 45^\circ$ or $\Delta\text{Dir}_w > 15^\circ$	15 %
H_s	$H_s > 0.46 \text{ m (1.5 ft)}$	15 %
T_p	$T_p > 3 \text{ sec}$	5 %
Lake level change	$> -0.15 \text{ m (6 in)}$	5 %
Storm	Occurred in past 12 hours	15 %
Visual	Flash rips identified	30 %

Likelihood	< 40 %	40 – 70 %	> 70 %
Tier	Low	Moderate	High

Table 2. Statistics of flash rip detection

Method \ Outcome	Correct detection	False alarm	Miss
RGB segmentation	55 %	32 %	13 %
HSV segmentation	75 %	16 %	9 %
Length threshold & HSV segmentation	83 %	8 %	9 %

Table 3. Summary for dates and conditions of flash rip occurrences and corresponding radar reflectivity images

Dates	Image	H_s (m)	T_p (sec)	U_w (m/s)	Dir_w	Reflectivity image
2016-06-26		0.49	4.0	6.7	SW	
2016-07-21		0.46	3.3	8.0	SW	
2016-08-24		0.91	3.3	5.8	SW	
2016-09-21		0.49*	4.1*	4.0	S	
2017-03-30		1.8*	7.1*	12	NE	
2017-07-12		0.67	4.1	6.7	SW	
2017-08-03		0.91	6.5	8.5	SW	
2017-10-03		0.76*	4.7*	5.8	SW	
2017-10-15		1.6*	6.7*	8.0	SW	

* indicates nearshore wave characteristics estimated from the NOAA National Data Buoy 45007 in Lake Michigan.